Arab J Sci Eng (2014) 39:3271–3277
DOI 10.1007/s13369-013-0940-3

RESEARCH ARTICLE - MECHANICAL ENGINEERING

Coating of AISI 1010 Steel by Ni–WC Using Plasma Transferred Arc Process

Gül Tosun

Received: 6 March 2012 / Accepted: 31 December 2012 / Published online: 13 February 2014

Abstract In the present study, mixed powders of 95 % Ni and 5 % WC were coated on the surface of AISI 1010 steel by plasma transferred arc process. The effect of current variation on the microstructure and hardness of the alloyed surfaces was investigated. After deposition, microstructural analyses including metallographic examination and microhardness measurements of the coatings were performed. The alloyed surfaces showed an increase in hardness when current was increased and this was attributed to the formation of hard phases. Upon solidification of the coating, different microstructures formed depending on the processing parameters. The microstructures of the alloyed surfaces consisted of widmanstatten ferrite, grain boundary ferrite, acicular ferrite, bainite and martensite.

Keywords Composite materials · Microstructure · Hardness

الخلاصة

تم - في هذه الدراسة - طلاء مساحيق مختلطة مكونة من 95٪ نيكل و5٪ كلوريد الخارصين على سطح صلب ايسي 1010 بوساطة عملية قوس نقل البلازما (PTA)، ودُرس تأثير اختلاف التيار في البنية المجهرية وصلابة الأسطح المسبوكة. وأجريت - بعد الترسيب - تحليلات الهيكلية المجهرية بما في ذلك فحص تكوينات المعادن وقياسات الصلادة الدقيقة للطلاء. وأظهرت السطوح المسبوكة زيادة في الصلادة عند زيادة التيار، ويعزى هذا إلى تشكل مراحل قاسية. وعند تصلب الطلاء، تشكلت هيكليات مجهرية مختلفة اعتمادا على معاملات المعالجة. وتتألف الهيكلية المجهرية للأسطح المسبوكة من فريت أيونات النيكل البلورية الطويلة، وحبوب حدود الفريت، وأسيكولار الفريت، وشكل بينايت الإبري وشكل الصلب البلوري القاسي مارتينسايت.

G. Tosun (✉)
Faculty of Technology, Department of Metallurgy and Materials Engineering, Firat University, 23119 Elazig, Turkey
e-mail: gultosun@firat.edu.tr

1 Introduction

Low carbon steels are generally preferred due to their low cost and easy machinability. However, due to low mechanical properties, hardness and corrosion resistance, their usage and application are restricted. The surfaces of these materials are coated to improve these properties [1]. There are several methods used in surface coating, one of which is plasma transferred arc (PTA) process. Recently, PTA weld surfacing has been applied to improve properties such as mechanical strength, wear, corrosion and heat resistance of material's surface due to its high deposition rate and lower heat input. With this method, it is possible to obtain metallurgical bonding between the coating layer and substrate material with very low dilution and distortion in numerous materials. The process provides such advantages as low cost surface, minimal dilution from the base metal, use of a lesser quantity of material and easy automation. Carbon, chromium or complex mixtures of metals and compounds may be used as alloying materials [2–8].

In this study, a mixture of tungsten carbide (WC) and Ti powders was used. WC used in this study is generally employed as a tool or die material. WC combines positive properties, such as high hardness, good wear resistance, a certain amount of plasticity and good wettability by molten metals considering other carbides. However, the brittleness and low formation heat make WC easily dissolvable by molten metals, which limits its usage as a structural material. Furthermore, clad tungsten carbide particles on a ductile material which are aimed to improve the wear performance of surface have the toughness of base material. The brittleness of WC-base composites restricts their usefulness in wear applications when a combination of high hardness and toughness is needed [6,7].

Bourithis et al. [1] studied the surface treatment of a tool steel by a PTA process. They showed that the wear resistance and hardness of specimens treated by PTA were better than the conventional heat-treated steel and the microstructure was mostly fine. Ozel et al. [2] investigated coating layer and interface coated with NiTi powder mixture on the surface of AISI 304 steel by PTA and observed that the coating thickness increased with current density and that the coating layer was poor in NiTi alloy with higher arc current densities. Hou et al. [3] studied microstructure and wear characteristics of cobalt-based alloy deposited by PTA weld surfacing. They observed that the as-welded coating consisted of a cobalt-based solid solution with face-centered cubic crystal structure and hexagonal $(Cr,Fe)_7C_3$. Bourithis and Papadimitriou [4] investigated the microstructure and the wear resistance of four different coatings (MMC-TiC, AISI M2, Fe–B, Fe–Cr–B) fabricated with PTA alloying technique. They observed that MMC-TiC coating showed good performance. Deuis et al. [5] reviewed a study on ferrous and non-ferrous base materials with metal-matrix composite coatings using different coating methods (PTA surfacing, laser cladding and thermal spraying). Alian and Jalham [8] performed a comparative work among three different types of coating materials to improve wear resistance of steel using plasma spray process. They investigated the effect of velocity, load and surface roughness for each coating type. Bourithis et al. [9] produced a metal matrix composite tool steel with TiC as reinforcing particles by PTA surface alloying of a construction carbon steel and investigated microhardness, microstructure and wear resistance of this alloyed surface. Bourithis and Papadimitriou [10] synthesized a high speed steel on the surface of a plain steel using PTA alloying technique. They observed layers with a fine cast microstructure consisting of a dendritic matrix of martensite/residual austenite embedded in a duplex M_6C and M_2C eutectic. Sudha et al. [11] investigated microchemistry and microstructure in a PTA weld overlay of Ni–Cr–Si–B alloy on AISI 304L stainless steel. They observed changes in microstructure, microchemistry and hardness based on the phase transitions of the Ni rich alloy during solidification and cooling on the base metal. Huang et al. [12] studied microstructure and properties of Cr_3C_2-modified nickel-based alloy coated with PTA process. They found that the γ(Ni, Fe), $M_7(C,B)_3$, Ni_4B_3, and $(Cr,Fe)_2B$ phases formed in the Cr_3C_2-free nickel-based alloy coating obtained with PTA process. Skarvelis and Papadimitriou [13] investigated PTA composite coatings with self-lubricating properties based on microstructure and tribological behavior of Fe and Ti sulfides. They observed that both TiC and MoS_2 ingredients dissolve completely in the melt under the plasma arc and that new compounds were formed during solidification. Liyanage et al. [14] studied microstructures and abrasive wear performance of Ni–WC coatings using different Ni-alloy chemistries by PTA. They observed the Ni–WC coatings with microstructures consisting of γNi dendrites with interdendritic Ni-based eutectics, borides and carbides. Xibao et al. [15] analyzed the thermal behavior of ceramic powders on the surface of a melting pool during PTA powder surfacing.

In this study, the surface of AISI 1010 steel was coated with a preform consisting of tungsten carbide/nickel powder mixture by using PTA. EDX, XRD and SEM analyses were employed to assess the compositions and microstructure of coating layer. The effects of the current on microstructure and microhardness of the coatings were also investigated.

2 Experimental Procedure

AISI 1010 steel with the dimensions of 100 × 20 × 10 mm and an initial hardness of 120–130 HV was chosen as the

Table 2 Characteristics of WC and Ni powders

Feature of coating material	Ni	WC
Purity (%)	99.8	99.5
Specific gravity (g/mol)	58.71	47.9
Powder dimension (mesh)	−325	70 μm
Melting temperature (°C)	1,453	2,870
Specific weight (g/cm^3)	8.9	4.507
Boiling temperature (°C)	2,832	6,000

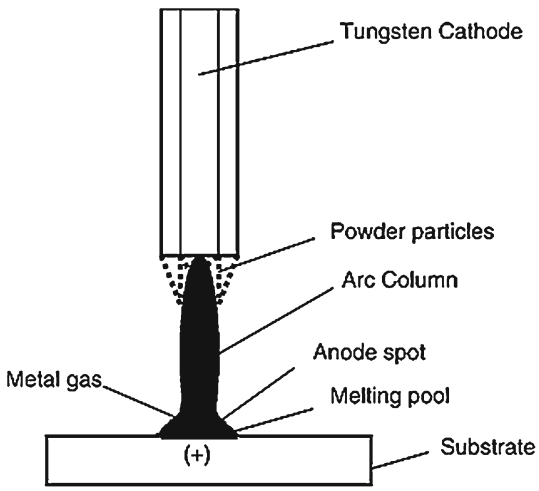

Fig. 1 Schematic drawing of the PTA powder surfacing [15]

Table 1 The chemical compositions of AISI 1010 steel

Element	C	Si	Mn	P	S	Cr	Ni	Cu	Nb	Ti	Fe
%	0.0807	0.3	0.347	0.0108	0.0146	0.0181	0.0196	0.0216	0.0009	0.0033	Remaining

Table 3 The experimental parameters and their values

Parameters	Values
Current, I (A)	120, 140, 160
Scan speed (mm/s)	1.2–1.5
Gas flow rate (l/min)	11
Shielding gas	99.9 % pure Argon
Electrode	2 % thorium tungsten
Electrode diameter (mm)	4.7
Voltage (V)	20
Plasma gas (m^3/h)	0.5
The distance between torch and material (mm)	2–4

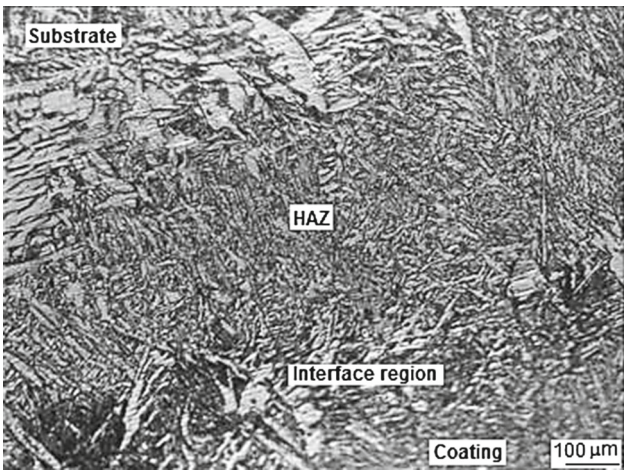

Fig. 2 Optic micrograph of coating layer, substrate, interface and HAZ

substrate material. The chemical compositions of AISI 1010 steel are shown in Table 1. Prior to cladding process, the substrate was polished with 400 grit SiC emery paper, cleaned and finally rinsed by acetone. The mixed powders of Ni and WC with 95 at.% Ni 5 at.% WC were blended for 12 h. The characteristic features of powders used are shown in Table 2. Later, the mixed powder layers in thickness of 1 mm were covered with a paste of the alloying powder by adding pure alcohol for the binding of powders. The binder was restricted within a limit to eliminate pore formation [16] and keep the powders on the surface under the flow of argon during the arc melting. The coated specimens were dried in a furnace at 60 °C for 1 h to enhance the adhesion effect between the coating material and the substrate. The operating principle of PTA melting used is schematically shown in Fig. 1. Surface coating procedure was realized in three different welding currents. The experimental parameter settings are shown in Table 3.

Specimens for metallographic examinations were taken from the cross section of the modified surface of coating areas. The metallographic specimens obtained were ground

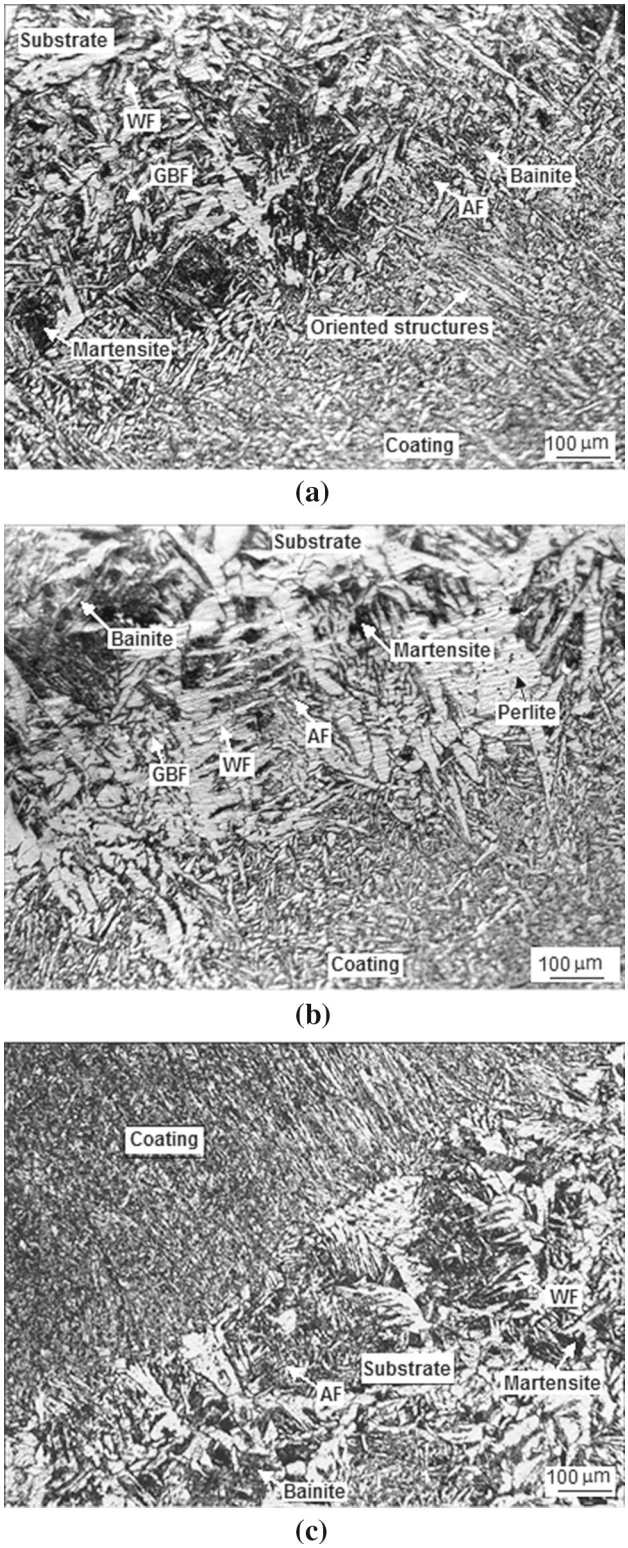

Fig. 3 Optical micrograph of HAZ microstructure, **a** 120 A, **b** 140 A, **c** 160 A

with 80–1200 mesh sandpaper; as a result, their surfaces were cleaned and then cross-sectional surfaces were polished by 3 µm diamond paste and solvent. For microstructural examina-

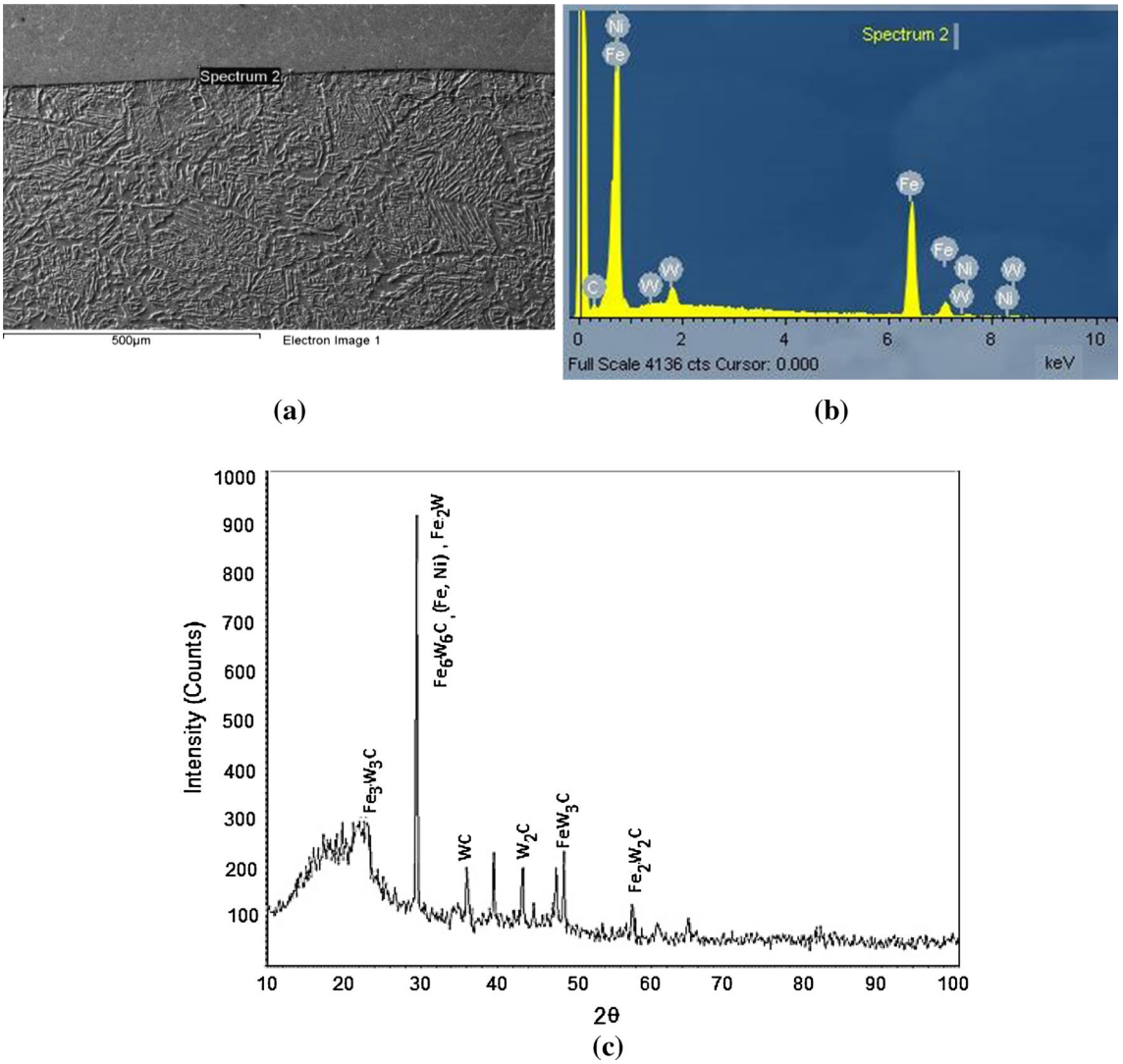

Fig. 4 **a** SEM micrograph of the specimen alloyed with $I = 120$ A, **b** EDS analysis taken on the point of number 4, **c** X-ray diffractogram

tion, the specimens were etched with 2 % Nital. Conventional characterization techniques such as optical (COIC XJP-6), scanning electron microscopy (SEM) and energy dispersive spectrograph (EDS) (JEOL JSM 7001F) were employed for studying the microstructure and elemental analysis of the alloyed zone. In addition, the microstructure, the effects of the current value on microhardness of the coatings were also investigated. Microhardness measurements were conducted by Leica microhardness tester under a load of 200 gf.

3 Results and Discussions

An almost uniform alloyed layer free of cracks and porosities was produced after the PTA melting process. It was observed that substrate layer with alloyed layer was perfectly adhered to each other. During coating process, four different regions occurred, namely coating layer, interface region, heat affected zone (HAZ) and substrate [2], which can be seen in Fig. 2. The diffusion coefficient of carbon in the carbide is much more than metal-forming carbide. Therefore, carbon diffuses much faster out of the carbide-forming metal carbide. Thus, if the diffusion activation energy is reached due to the difference in the rate of diffusion, the carbide undergoes decarburization and an interfacial region occurs [17].

During coating process, the surface is subjected to high temperatures which also affects both substrate material and coating material. The energy of PTA melts the surface of the substrate and the powder layer together and provides an alloyed surface. Therefore, liquation can be seen along the grain boundary in a region very close to the fusion boundary. Probably, the liquid formed solidifies in two directions,

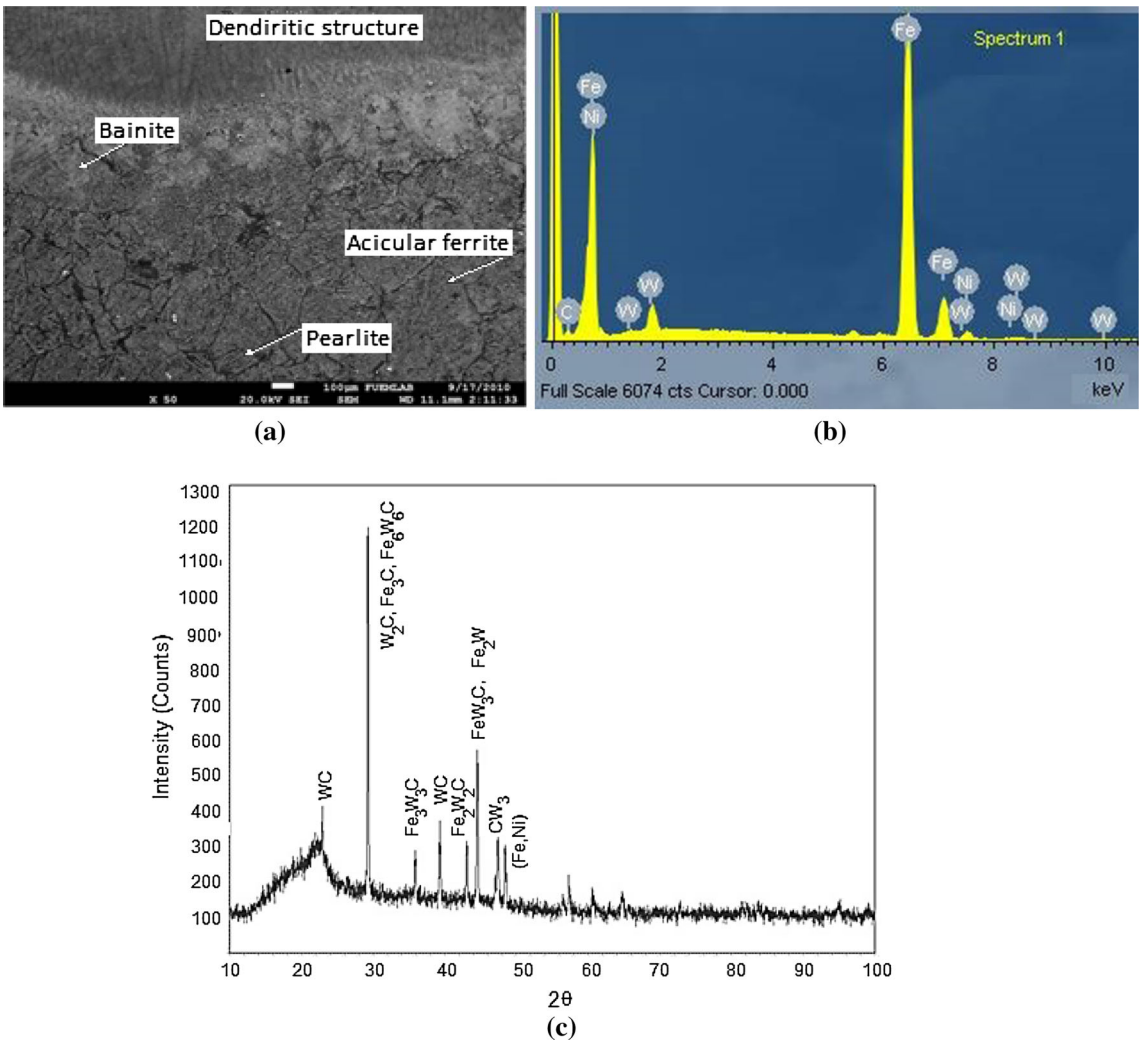

Fig. 5 **a** SEM micrograph of the specimen alloyed with $I = 160$ A, **b** EDS analysis taken on the point of number 4, **c** X-ray diffractogram

parallel and perpendicular to the heat flow [3,9,15]. Element transitions occurred in both sides. The elements from the substrate changed the composition and structure of the transition zone in the proximity of the substrate [18]. Alloyed layer joined as a result of the melting of a thin layer of the substrate material. As a result, the variations in microstructure occurred. In addition, from the microstructures of the layers with Ni/WC after the process, it was seen that microstructures solidified in varying composition by the process parameters such as energy input values.

When the low current is chosen, heat input decreases, implying a high cooling rate, which is concluded by rapid solidification. As a result, martensite phase occurred. The bainitic structure around the larger martensite islands occurred along the grain boundaries, which were surrounded by ferrite grains. As a result, acicular ferrite was observed (Fig. 3a). Similar results can be found in the literature [19].

It was observed that the dendritic structures occurred perpendicular to the welding axis on coating side at all coatings. A reason for the occurrence of the dendritic structure is the huge difference between the melting points of Ni and other phases formed by tungsten carbide dissolution [16]. The amount of W in the dendrites was low. Since dendrites are the first to be solidified; the extra W in the melt generally solidifies in only eutectic areas. The dominant phases in microstructure of substrate material were martensite and bainite. Depending on the rate of cooling, grain boundary ferrite (GBF), widmanstatten type ferrite (WF), acicular (needle-like) ferrite (AF) and a negligible amount of martensite with austenite and decomposed pearlite phase occurred. In low carbon steels, it was not demanded that presence of WF and GBF caused grain coarsening in HAZ. The presence of GBF which depends on the amount of WF is the reason for the loss of toughness and brittle cracking in the weld. The nucleation of AF, usually due to the non-metallic inclusions, improves

the material toughness and strength. The bainite microstructure in steel with low carbon is very similar to that of AF and, therefore, it is very difficult to distinguish between these phases [19].

It was observed that, when current increased to 140 A from 120 A, amount of widmanstatten type ferrite, bainite, AF and GBF increased and amount of martensite decreased (Fig. 3b). In coating side, refined dendritic structures were observed. When current increased to 160 A from 140 A, the amount of WF and martensite decreased, the amount of AF and bainite increased and pearlite occurred. Furthermore, it was observed that AF and bainite islands occurred. Dendritic structures on coating side were refined with higher current (Fig. 3c). When the current increased, a slower solidification occurs with heat input increased. The more heat is incorporated into the MMC, the longer it takes to cool down. Higher cooling rate is based on the higher energy input during welding process which resulted in grain refinement [5,18].

Considering W–Fe–C phase diagram, it can be asserted that WC + α-Fe + hexagonal (M_6C) phases can be probably formed. In the microstructure of the surface modified material, WC and W_2C types, most of which were M_6C (M = W, Fe) carbides, were determined together with austenitic hypoeutectic structure. The formation of FeW_3C and Fe_6W_6C (Fig. 4) indicates the significance of a small amount of melted iron from the substrate in the microstructure of the coating. The XRD analysis of the alloyed surface at low current was given in Fig. 4. It was observed that Fe_3C, Fe_2W, Fe_6W_6C, CW_3, WC, FeW_3C phases occurred. Whereas, it was also viewed that a lot of Fe, Ni, CW_3, WC, Fe_2W, Fe_3C, $FeNi_3$, Fe_3W_3C, Fe_2W_2C, FeW_3C, Fe_6W_6C, W_2C occurred at high current rates (Fig. 5).

Through the coating layer, hardness varied between 195 and 302 HV and decreased progressively in depth (Fig. 6). Hardness increased with the increasing current. When current is increased, it is expected to decrease the level of hardness, which can simply be attributed to WF, considerable amount of AF and some bainite formation [19]. The refinement of grain structure showed improvement in the hardness. It is expected that hardness would decrease with bainite formation. The hardness increased with the formation of acicular ferrite islands in the structure.

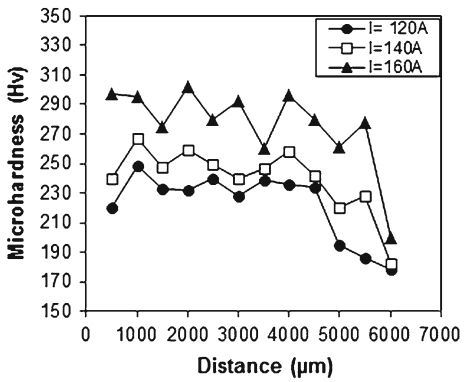

Fig. 6 Effect of current on the microhardness

4 Conclusions

- In this study, AISI 1010 steel was coated with Ni–WC powder by PTA successfully.
- At low current, bainitic structure around the larger martensite islands occurred along the grain boundaries which were surrounded by ferrite grains and acicular ferrite was observed. When the current was increased to 140 A from 120 A, amount of widmanstatten type ferrite, bainite, AF and GBF increased and amount of martensite decreased. When the current was increased to 160 A from 140 A, the amount of WF and martensite decreased, amount of AF and bainite increased and pearlite occurred. Furthermore, it was also observed that AF and bainite islands occurred.
- Fe_3C, Fe_2W, Fe_6W_6C, CW_3, WC, FeW_3C phases occurred at low current value, whereas a considerable amount of Fe,Ni, CW_3, WC,Fe_2W, Fe_3C, $FeNi_3$, Fe_3W_3C, Fe_2W_2C, FeW_3C, Fe_6W_6C, W_2C occurred at high current value.
- When the current was increased, the hardness increased due to formation of acicular ferrite islands in the structure.
- Through the coating region, the hardness increased with the increasing energy input.

References

1. Bourithis, E.; Tazedakis, A.; Papadimitriou, G.A.: A study on the surface treatment of “Calmax” tool steel by a plasma transferred arc (PTA) process. J. Mater Process Technol. **128**, 169–177 (2002)
2. Ozel, S.; Kurt, B.; Somunkiran, I.; Orhan, N.: Microstructural characteristic of NiTi coating on stainless steel by plasma transferred arc process. Surf. Coat. Technol. **202**, 3633–3637 (2008)
3. Hou, Q.Y.; Gao, J.S.; Zhou, F.: Microstructure and wear characteristics of cobalt-based alloy deposited by plasma transferred arc weld surfacing. Surf. Coat. Technol. **194**, 238–243 (2005)
4. Bourithis, L.; Papadimitriou, G.D.: The effect of microstructure and wear conditions on the wear resistance of steel metal matrix composites fabricated with PTA alloying technique. Wear **266**, 1155–1164 (2009)
5. Deuis, R.L.; Yellup, J.M.; Subramanian, C.: Metal-matrix composıte coatings by PTA surfacing.Compos SciTechnol **58**, 299–309 (1998)
6. Harsha, S.; Dwivedi, D.K.; Agrawa, A.: Influence of WC addition in Co–Cr–W–Ni–C flame sprayed coatings on microstructure, microhardness and wear behavior. Surf. Coat. Technol. **201**, 5766–5775 (2007)
7. Zhou, S.; Huang, Y.; Zeng, X.: A study of Ni-based WC composite coatings by laser induction hybrid rapid cladding with elliptical spot.Appl. Surf. Sci. **254**, 3110–3119 (2008)

8. Alian, A.; Jalham, I.S.: Abrasive wear resistance comparative study of plasma- sprayed steel by magnesıum zirconate, aluminum-bronze, molybdenum, and mixtures of them as coating materials.Arab. J. Sci. Eng. **31**(1B), 27–34 (2006)
9. Bourithis, L.; Milonas, A.; Papadimitriou, G.D.: Plasma transferred arc surface alloying of a construction steel to produce a metal matrix composite tool steel with TiC as reinforcing particles. Surf. Coat. Technol. **165**, 286–295 (2003)
10. Bourithis, L.; Papadimitriou, G.D.: Synthesizing a class "M" high speed steel on the surface of a plain steel using the plasma transferred arc (PTA) alloying technique: microstructure and wear properties. Mat. Sci. Eng. A **361**, 165–172 (2003)
11. Sudha C.; Shankar, P.; SubbaRao, R.V.; Thirumurugesan, R.; Vijayalakshmi, M.; Raj, B.: Microchemical and microstructural studies in a PTA weld overlay of Ni–Cr–Si–B alloy on AISI 304L stainless steel. Surf. Coat. Technol. **202**, 2103–2112 (2008)
12. Huang, Z.; Hou, Q.; Wang, P.: Surface Microstructure and properties of Cr3C2-modified nickel-based alloy coating deposited by plasma transferred arc process. Surf. Coat. Technol. **202**, 2993–2999 (2008)
13. Skarvelis, P.; Papadimitriou, G.D.: Plasma transferred arc composite coatings with self-lubricating properties, based on Fe and Ti sulfides: microstructure and tribological behavior. Surf. Coat. Technol. **203**, 1384–1394 (2009)
14. Liyanage, T.; Fisher, G.; Gerlich, A.P.: Microstructures and abrasive wear performance of PTAW deposited Ni–WC overlaysusing different Ni-alloy chemistries. Wear 274–275, 345–354 (2012)
15. Xibao, W.; Chunguo, L.; Xiaomin, P.; Libo, S.; Hong, Z.: The powder's thermal behavior on the surface of the melting pool during PTA powder surfacing. Surf. Coat. Technol. **201**, 2648–2654 (2006)
16. Buytoz, S.: Microstructural properties of SiC based hardfacing on low alloy steel. Surf. Coat. Technol. **200**, 3734–3742 (2006)
17. Just, C.H.; Badisch, E.; Wosik, J.: Influence of welding current on carbide/matrix interface properties in MMCs. J. Mater Process Technol. **210**, 408–414 (2010)
18. Eroglu, M.: Boride coatings on steel using shielded metal arc welding electrode: microstructure and hardness. Surf. Coat. Technol. **203**, 2229–2235 (2009)
19. Gural, A.; Bostan, B.; Ozdemir, A.T.: Heat treatment in two phase region and its effect on microstructure and mechanical strength after welding of a low carbon steel. Mater Design **28**, 897–903 (2007)